

# Macropinocytosis of Nab-paclitaxel Drives Macrophage Activation in Pancreatic Cancer

Jane Cullis<sup>1</sup>, Despina Siolas<sup>1</sup>, Antonina Avanzi<sup>1</sup>, Sugata Barui<sup>2</sup>, Anirban Maitra<sup>2</sup>, and Dafna Bar-Sagi<sup>1</sup>

## Abstract

Pancreatic cancer is a devastating disease that is largely refractory to currently available treatment strategies. Therapeutic resistance is partially attributed to the dense stromal reaction of pancreatic ductal adenocarcinoma tumors that includes a pervasive infiltration of immunosuppressive (M2) macrophages. Nab-paclitaxel (trade name Abraxane) is a nanoparticle albumin-bound formulation of paclitaxel that, in combination with gemcitabine, is currently the first-line treatment for pancreatic cancer. Here, we show that macrophages internalized nab-paclitaxel via macropinocytosis. The macropinocytic uptake of nab-paclitaxel

induced macrophage immunostimulatory (M1) cytokine expression and synergized with IFN $\gamma$  to promote inducible nitric oxide synthase expression in a TLR4-dependent manner. Nab-paclitaxel was internalized by tumor-associated macrophages *in vivo*, and therapeutic doses of nab-paclitaxel alone, and in combination with gemcitabine, increased the MHCII<sup>+</sup>CD80<sup>+</sup>CD86<sup>+</sup> M1 macrophage population. These data revealed an unanticipated role for nab-paclitaxel in macrophage activation and rationalized its potential use to target immune evasion in pancreatic cancer. *Cancer Immunol Res*; 5(3); 182–90. ©2017 AACR.

## Introduction

Pancreatic ductal adenocarcinoma (PDAC) is a lethal disease with a 5-year survival rate of less than 6%. A defining feature of PDAC is its prominent desmoplastic reaction with an extensive leukocytic infiltration dominated by macrophages (1). Depending on signals that prevail within their microenvironment, macrophages can adopt a variety of functional states. In response to bacterial products such as lipopolysaccharide (LPS) and Th1 cytokines, macrophages become immunostimulatory (M1). M1 macrophages are characterized by high expression of nitric oxide synthase (iNOS), MHC class II (MHCII) proteins, CD80, CD86, and TNF $\alpha$ , and can exert tumoricidal effects (2). In contrast, in the presence of Th2 cytokines, macrophages acquire an alternatively activated state (M2) that is immunosuppressive, tumor promoting, and is characterized by the expression of Arginase 1, CD206, and low amounts of MHCII (2). Although tumor-associated macrophages (TAM) in the pancreas exhibit both M1 and M2 phenotypes, higher M2:M1 ratios correlate with disease progression and shorter survival in patients (1, 3).

Abraxane (nab-paclitaxel) is a nanoparticle albumin-bound formulation of paclitaxel that, in combination with gemcitabine, is currently the first-line treatment for pancreatic cancer (4). The

primary mechanism of antineoplastic activity of paclitaxel is its ability to stabilize microtubules and prevent cell division of rapidly dividing tumor cells. However, in macrophages, paclitaxel can exert cell-cycle-independent effects by acting as an LPS mimetic and inducing M1 polarization in a Toll-like receptor 4 (TLR4)-dependent manner (5–7). We therefore sought to investigate the effects of nab-paclitaxel on macrophage polarization. We report that nab-paclitaxel is internalized by macrophages principally via macropinocytosis and is sufficient to drive macrophage M1 polarization *in vitro* and *in vivo*. These data reveal a previously unappreciated mechanism of action of nab-paclitaxel and suggest that nab-paclitaxel may co-operate with immunotherapeutic agents to restore immune recognition in PDAC.

## Materials and Methods

### Cell lines and cell culture treatments

All cells were maintained under 5% CO<sub>2</sub> at 37°C and cultured in DMEM (Gibco) supplemented with 10% FBS (Gibco), penicillin and streptomycin (Gibco), and 25 mmol/L HEPES (Gibco). Mouse RAW 264.7 cells were obtained from the American Type Culture Collection (2014, ATCC TIB-71). Mouse KPC cells were a kind gift from Dr. R.H. Vonderheide (2013) and generated as previously described (8). Cell lines were not authenticated and were tested for *mycoplasma* contamination every 3 months by DAPI stain of cells grown for 1 week in the absence of antibiotics. KPC and RAW 264.7 were propagated for 2 to 3 passages (approximately 1 week) prior to use in all experiments and were kept in culture for no longer than 1 month. Recombinant mouse IFN $\gamma$  was purchased from R&D Systems (CN 485 MI/CF), LPS (L2630) and paclitaxel (T7402) were purchased from Sigma-Aldrich, CLI-095 was purchased from Invivogen (TLRL-CLI95), BAPTA-AM was purchased from Life Technologies (B6769), and 5-(N-ethyl-N-isopropyl) amiloride (EIPA) was purchased from Invitrogen Molecular Probes (e-3111). Reagents were used at concentrations

<sup>1</sup>Department of Biochemistry and Molecular Pharmacology, New York University School of Medicine, New York, New York. <sup>2</sup>Departments of Pathology and Translational Molecular Pathology, University of Texas MD Anderson Cancer Center, Houston, Texas.

**Note:** Supplementary data for this article are available at Cancer Immunology Research Online (<http://cancerimmunolres.aacrjournals.org/>).

**Corresponding Author:** Dafna Bar-Sagi, New York University School of Medicine, 530 First Avenue, Executive Offices, HCC-15th Floor, New York, NY 10016. Phone: 212-263-2095; Fax: 646-501-6721; E-mail: [dafna.bar-sagi@nyumc.org](mailto:dafna.bar-sagi@nyumc.org)

**doi:** 10.1158/2326-6066.CIR-16-0125

©2017 American Association for Cancer Research.

of 5 ng/mL (IFN $\gamma$ ), 20 ng/mL (LPS), 10  $\mu$ mol/L (paclitaxel), 500 nmol/L (CLI-095), 50  $\mu$ mol/L (BAPTA-AM), and 50  $\mu$ mol/L (EIPA) unless indicated otherwise. Tetramethylrhodamine (TMR)-labeled dextran was purchased from Invitrogen (D1822). Nab-paclitaxel (Abraxane; Abraxis BioScience) pharmaceutical grade powder was purchased through the NYU Langone Medical Center pharmacy and used at a concentration of 10  $\mu$ mol/L for *in vitro* experiments.

### Antibodies

Antibodies used for Western blotting are as follows: rabbit anti-IL1 $\alpha$ , rabbit anti-IL1 $\beta$  (Abcam ab9722), rabbit anti-IL6 (Novus Biologicals NB600-1131), rabbit anti-iNOS (Cell Signaling Technology, CST 13120), rabbit anti-TNF $\alpha$  (Abcam ab9739), and mouse anti-VINCULIN (Sigma V9131). F4/80 antibody used for immunofluorescence and immunohistochemistry was purchased from eBiosciences (rat anti-mouse F4/80, clone BM8, ref 14-4801-82). CD16/CD32 antibody was purchased from BD Biosciences (rat anti-mouse-CD16/CD32, clone 2.4G2) and used at a concentration of 25  $\mu$ g/mL. Monoclonal antibodies used for flow cytometry were all purchased from Biolegend unless indicated otherwise: anti-CD45 (Brilliant Violet 421-anti-mouse-CD45, clone 30-F11), anti-F4/80 (PE-anti-mouse-F4/80, clone BM8 or APC-anti-mouse-F4/80, clone BM8), anti-MHCII (FITC-anti-mouse-I-A/I-E, clone M5/114.15.2, BD Biosciences), anti-CD80 (PE/Cy7-anti-mouse-CD80, clone 16-10A1), anti-CD86 (PerCP-anti-mouse-CD86, clone GL-1), and anti-IL1 $\alpha$  (PE-anti-mouse-IL1 $\alpha$ , clone ALF-161).

### Western blot analysis

Western blot analyses were initiated 24 hours (iNOS) or 8 hours (IL1 $\alpha$ , IL1 $\beta$ , IL6, and TNF $\alpha$ ) following cell culture treatments. Total cell lysates were harvested in sample buffer (40 mmol/L Tris, pH 6.8, 1% SDS, 5% beta-mercaptoethanol, 7.5% glycerol, and 0.01% bromophenol blue) and incubated at 99°C for 5 minutes. Cell lysates (1/10 of total volume) were loaded onto 10% SDS-Polyacrylamide gels for electrophoresis and transferred onto nitrocellulose membranes for 1 hour at 100 volts at 4°C. Membranes were blocked for 1 hour at room temperature in 5% BSA (Sigma-Aldrich) diluted in PBS containing 0.1% Tween 20 prior to immunodetection.

### Gene expression analysis

For *in vitro* qPCR analysis, total RNA was harvested 2 hours (IL1 $\alpha$ , IL1 $\beta$ , IL6, TNF $\alpha$ , and iNOS) or 8 hours (IL12 $\beta$ ) after cell culture treatments, using the QIAGEN RNA extraction Kit (QIAGEN). For *in vivo* gene expression analysis, the CD45<sup>+</sup>F4/80<sup>+</sup> double-positive population was sorted directly into TRIzol LS Reagent (Thermo-Fisher Scientific; CN 10296) from dissociated orthotopic tumors 48 hours after treatment, and total RNA was purified according to the manufacturer's protocol. Purified RNA (1  $\mu$ g) was reverse-transcribed using the QuantiTect Reverse Transcription Kit (QIAGEN), and 1 of 10 of cDNA mixture (*in vitro* experiments) or 1 of 3 of cDNA mixture (*in vivo* experiments) was used for qPCR reaction. Primers were obtained from Integrated DNA Technologies (IDT) with the following sequences (5'-3'): *Il1a* (Forward) AATCAAGATGGCCAAAGTTCC, (Reverse) ATTCAGAGAGATGGTCAATGG; *Il1b* (Forward) GCAACTGTTCTGAACTCAACT, (Reverse) ATCTTTGGGGTCCGTCAACT; *Il6* (Forward) TAGTCCTTCTACCCCAATTTCC, (Reverse) TTGGTCCTTAGCCACTCCTTC; *Inos*

(Forward) GTTCTCAGCCCAACAATACAAGA, (Reverse) GTGGA-CGGGTCGATCTCAC; *Tnfa* (Forward) CTGTAGCCACGTCGTAGC, (Reverse) TTGAGATCCATGCCGTTG; *Il12b* (*Il12 p40*) (Forward) TGGTTTGCCATCGTTTGGCTG, (Reverse) ACAGGTGAGGTTCACTGTTTCT; *Gapdh* (Forward) CACGGCAAATTCACGG-CACAGTC, (Reverse) ACCCGTTTGGCTCCACCCTTCA; *Rps29* GTCTGATCCGCAAATACGGG (Forward), AGCCTATGTCCTTC-CGGTACT (Reverse).

### Synthesis of Oregon green-labeled paclitaxel and nab-paclitaxel

Albumin-bound Oregon Green 488-labeled paclitaxel (OG-nab-paclitaxel) was prepared by coupling Oregon Green 488-labeled paclitaxel (OG-paclitaxel; Thermo Fisher Scientific, CN P22310) to human serum albumin (Sigma-Aldrich; CN 05420). Briefly, 0.9 mg OG-paclitaxel was dissolved in 64.8  $\mu$ L chloroform and 7.2  $\mu$ L ethanol and added to 18 mg human serum albumin dissolved in 3.6 mL water with vigorous stirring. The suspension was sonicated at 40% amplitude for 4 cycles of 1 minute each with 30-second intervals. The organic solvent was then evaporated using rotavapor at 40°C. The resulting suspension was distributed equally into glass vials and lyophilized to obtain dry OG-nab-paclitaxel amenable to long-term storage at -20°C.

### Macropinocytosis assays

Macropinocytosis assays, image acquisition, image processing tools, and macropinosome quantification were performed as previously described (9). For *ex vivo* nab-paclitaxel uptake assays, orthotopic tumors were cut into approximately 3 mm  $\times$  3 mm sections and incubated for 20 minutes at 37°C in serum-free medium containing Oregon Green-labeled nab-paclitaxel (0.5 mg/mL). Tumor sections were then washed once with PBS at room temperature and immediately embedded in Tissue-Tek OCT medium (VWR) and fixed for 1 hour on dry ice. Fixed tumor sections were stored at -80°C until cryosectioned and mounted on coverslips to be stained for immunofluorescence.

### Immunohistochemistry

Immunohistochemistry on tumor sections was performed as previously described (10).

### Cell sorting and flow cytometry

Staining for cell sorting and flow cytometry analysis was performed by incubating single-cell suspensions with primary fluorochrome-labeled antibodies on ice for 30 minutes. For cell sorting, cells were washed once with FACS buffer (PBS supplemented with 1% FBS) and immediately sorted on an SY2300 cell sorter (Sony). For flow cytometry, cells were fixed in 3.7% formaldehyde diluted in FACS buffer overnight at 4°C prior to analysis. For IL1 $\alpha$  staining, cells were permeabilized and fixed with FoxP3/Transcription Factor Staining Buffer Set (eBioscience CN00-5523) for 45 minutes at 4°C and stained overnight at 4°C. All samples were washed once with FACS buffer prior to analysis on an LSRII UV flow cytometer (BD Biosciences). Collected data were analyzed using FlowJo data analysis software (V10).

### Animal studies

All animals used in this study were 8-week-old C57/BL6 female mice purchased from Charles River Laboratories. For orthotopic

implantations,  $1 \times 10^5$  KPC cells were resuspended in 20  $\mu$ L cold PBS and mixed with 20  $\mu$ L Matrigel (Corning; ref 254348) prior to injection into the pancreas of syngeneic mice. After 2 weeks, orthotopically implanted mice were treated intraperitoneally with gemcitabine (120 mg/kg, Gemzar, Eli Lilly) and nab-paclitaxel (120 mg/kg, Abraxane; Abraxis Bioscience) resuspended in sterile PBS. Both drugs were purchased through the NYU Langone Medical Center pharmacy. All animal care and procedures were approved by the Institutional Animal Care and Use Committee at the NYU School of Medicine.

### Statistical analyses

Statistical comparisons were evaluated by the Student *t* test. All *P* values stated are intentionally presented as uncorrected for multiple comparisons, as one planned comparison was conducted for each experimental condition tested (i.e., multiple comparisons were not performed).

## Results

### Macrophages internalized nab-paclitaxel via macropinocytosis

Macrophages undergo constitutive macropinocytosis, a form of nonselective fluid-phase endocytosis that, together with receptor-activated phagocytosis, regulates antigen sampling and scavenging of invading pathogens (11). Macropinocytosis is also an established route of internalization of many nanoparticle formulations (12). Given that macrophages constitute a dominant immune infiltrate in PDAC, we set out to assess the extent and mode of nab-paclitaxel internalization by macrophages. To this end, the macrophage cell line RAW 264.7 was incubated with high molecular weight TMR-labeled dextran (TMR-dextran), an established marker of macropinosomes, and Oregon Green-labeled nab-paclitaxel (OG-nab-paclitaxel). OG-nab-paclitaxel localized predominantly to dextran-positive macropinosomes (Fig. 1A). Furthermore, OG-nab-paclitaxel internalization was reduced following treatment with the macropinocytosis inhibitor 5-[N-ethyl-N-isopropyl] amiloride (EIPA), indicating that nab-paclitaxel internalization depended on a macropinocytotic uptake mechanism (Fig. 1B). To determine the contribution of phagocytosis to nab-paclitaxel internalization, we tested the requirement of Fc receptors for uptake because, unlike other major phagocytic receptor families, Fc receptors are constitutively active in macrophages (13). Inhibition of Fc receptors I and III with blocking antibodies to CD16 and CD32 (14) did not affect the internalization of OG-nab-paclitaxel (Fig. 1C). Moreover, depletion of intracellular calcium, required for constitutive macropinocytosis but not Fc receptor-dependent phagocytosis in macrophages (15, 16), effectively blunted OG-nab-paclitaxel uptake (Fig. 1D). Together, these data demonstrate that nab-paclitaxel is internalized by macrophages predominantly via macropinocytosis.

### Macropinocytosis of nab-paclitaxel drove M1 macrophage activation *in vitro* via TLR4

Consistent with recent findings by Tanei and colleagues (17), we did not observe significant cytotoxic effects of nab-paclitaxel on macrophages at concentrations required for its internalization (data not shown). Therefore, we assessed the capacity of nab-paclitaxel to induce macrophage M1 activation. Because paclitaxel promotes M1 polarization by acting as an LPS mimetic (18), we evaluated the effect of nab-paclitaxel treatment on the induction

of a panel of LPS-inducible cytokines. Treatment of RAW 264.7 cells with nab-paclitaxel was sufficient to induce the gene expression of *Il1a*, *Il1b*, *Il6*, *Il12b* (*Il12 p40*), and *Tnfa* in a similar manner to free paclitaxel (Fig. 2A). Nab-paclitaxel also increased IL1 $\alpha$ , IL1 $\beta$ , IL6, and TNF $\alpha$  protein expression to a similar extent as LPS (Supplementary Fig. S1). Nab-paclitaxel-dependent M1 cytokine expression was inhibited by EIPA and BAPTA-AM, but not by blocking antibodies to the Fc I and III receptors, demonstrating that macropinocytosis was required for its LPS mimetic effects (Fig. 2B). The tumor cell inhibitory function of M1 macrophages is partially attributed to the upregulation of inducible nitric oxide synthase (iNOS), an enzyme that catalyzes the production of tumor cell cytotoxic nitric oxide from L-Arginine (19). It has been shown that LPS synergizes with IFN $\gamma$  to induce iNOS protein expression in macrophages (20, 21). Similarly, nab-paclitaxel treatment induced robust iNOS expression in the presence of IFN $\gamma$  (Fig. 2C). The expression of the nab-paclitaxel-driven iNOS gene and protein was partially inhibited by EIPA (Fig. 2D), further supporting the idea that macropinocytosis of nab-paclitaxel contributes to its M1 polarizing effects. Paclitaxel induces macrophage activation via binding to myeloid differentiation factor 2 (MD2), an adaptor protein to TLR4 (18). Indeed, we found that the TLR4 inhibitor CLI-095 abrogated nab-paclitaxel and LPS-dependent *Il1a*, *Il1b*, *Il6*, *Il12b*, and *Tnfa* gene expression (Fig. 3A and Supplementary Fig. S2) and iNOS protein expression (Fig. 3B). These results indicate that nab-paclitaxel signals through the TLR4 receptor.

### Nab-paclitaxel induced M1 activation in pancreatic TAMs *in vivo*

Next, we sought to determine whether nab-paclitaxel could induce M1 polarization of macrophages in the pancreatic tumor microenvironment. To this end, we employed an orthotopic model of PDAC in which cells isolated from primary pancreas tumors of *Kras<sup>LSL-G12D/+</sup>*, *Trp53<sup>LSL-R172H/+</sup>*, *Pdx1-Cre* (KPC) transgenic mice were surgically implanted into the pancreas of immunocompetent syngeneic wild-type animals. In this model, the cells formed tumors within 2 weeks after implantation and exhibited an extensive F4/80<sup>+</sup> macrophage infiltrate (Fig. 4A). To determine whether TAMs can internalize nab-paclitaxel, we incubated pancreatic tumors with OG-nab-paclitaxel and found that F4/80<sup>+</sup> cells within the tumor took up nab-paclitaxel (Fig. 4B). Moreover, 83% of CD45<sup>+</sup> F4/80<sup>+</sup> cells isolated from KPC orthotopic tumors by FACS internalized OG-nab-paclitaxel following *ex vivo* treatment (Supplementary Fig. S3A). To determine whether nab-paclitaxel internalization induces M1 polarization of pancreatic tumor-associated macrophages *in vivo*, we treated orthotopic tumor-bearing mice with a single therapeutic dose of nab-paclitaxel, alone or in combination with gemcitabine, and analyzed the functional activation of macrophages within the tumor 48 hours after treatment (Fig. 4C). Optimal macrophage activation by immunogenic stimuli requires both the upregulation of antigen-presenting MHCII molecules and the induction of T-cell costimulatory molecules CD80 and CD86 at the cell surface (22). Analysis of the MHCII<sup>+</sup>CD80<sup>+</sup>CD86<sup>+</sup> cell population by flow cytometry revealed that single-agent nab-paclitaxel was sufficient to increase the MHCII<sup>+</sup>CD80<sup>+</sup>CD86<sup>+</sup> macrophage population within the tumors compared with vehicle-treated mice, with no change in total macrophage numbers across treatment cohorts (Fig. 4C and Supplementary Fig. S3B). Nab-paclitaxel treatment also induced an increase in IL1 $\alpha$  protein

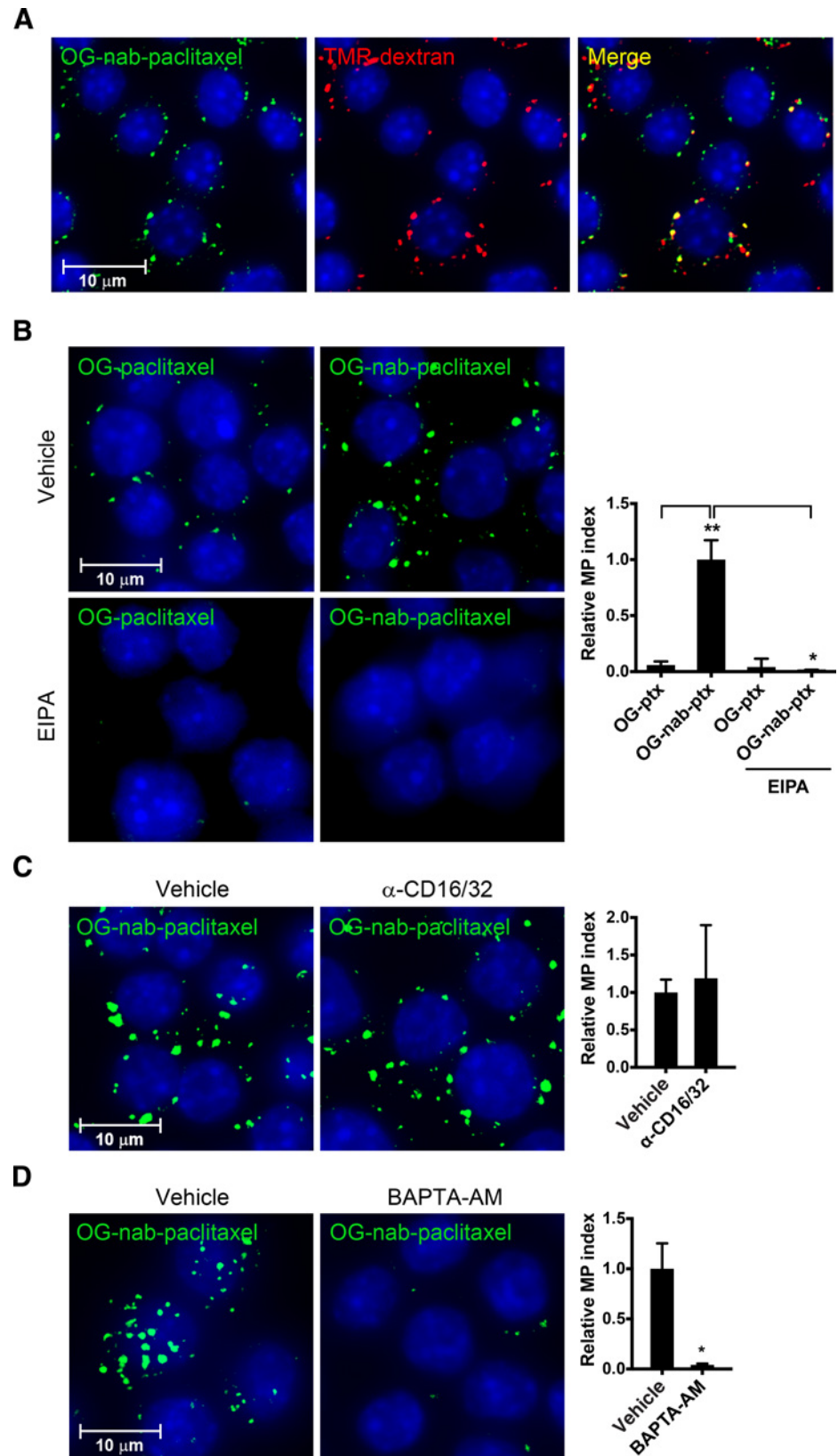


**Figure 1.** Macrophages internalize nab-paclitaxel via macropinocytosis. Immunofluorescent analysis of RAW 264.7 cells treated for 30 minutes with (A) OG-nab-paclitaxel and TMR-dextran, (B) OG-paclitaxel (left) or OG-nab-paclitaxel (right) and DMSO (vehicle, top) or pretreated with 100 μmol/L EIPA (bottom), (C) OG-nab-paclitaxel and PBS (vehicle) or pretreated with anti-CD16/CD32, and (D) OG-nab-paclitaxel with DMSO (vehicle) or with BAPTA-AM. All pretreatments were 30 minutes. Macropinocytosis indices are represented graphically in B-D (right) with bars indicating the SE from at least three independent experiments. \*,  $P < 0.05$ ; \*\*,  $P < 0.01$ .

Downloaded from <http://aacrjournals.org/cancerimmunolres/article-pdf/5/3/182/235116/182.pdf> by guest on 22 May 2025

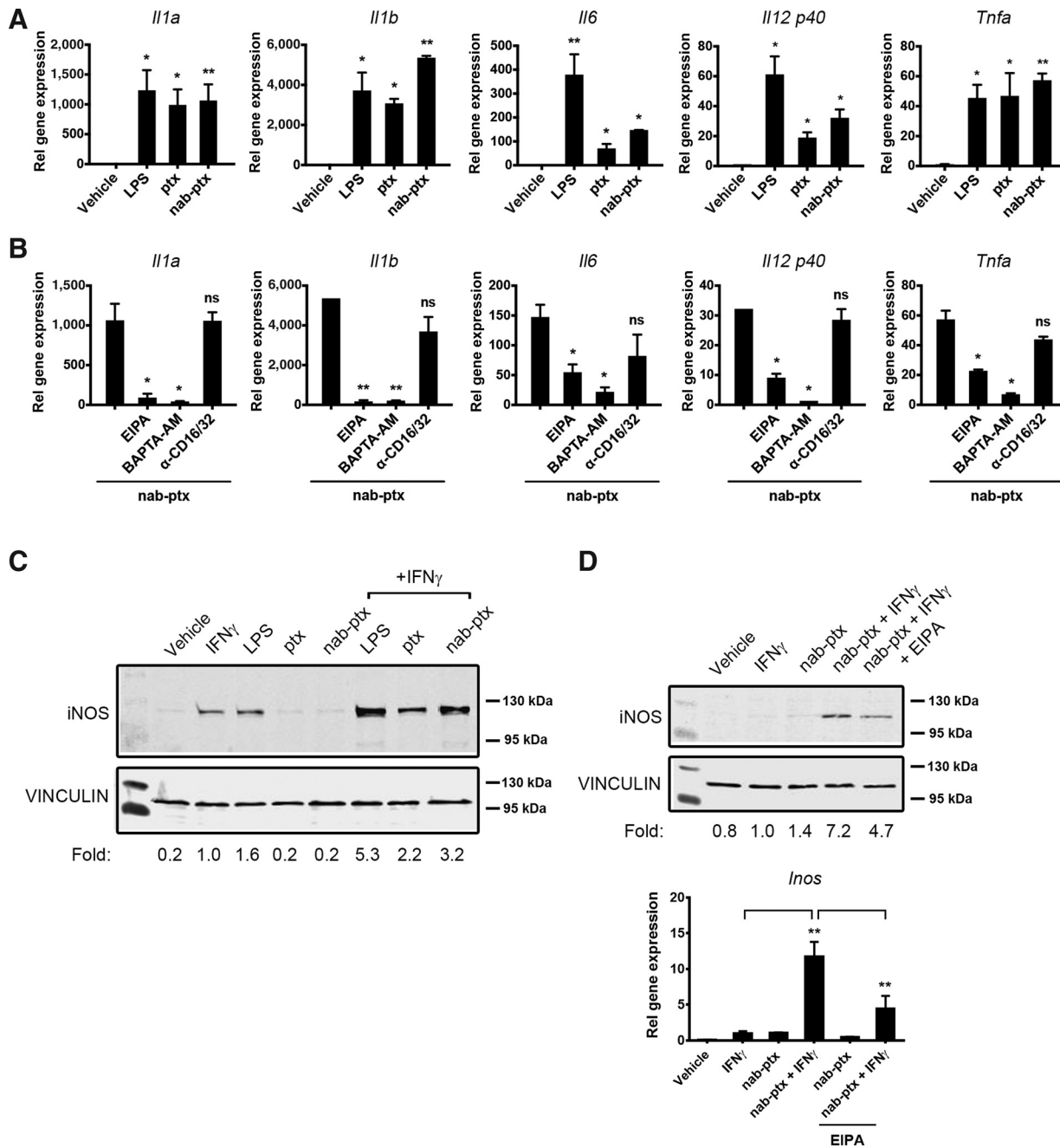


**Figure 2.** Nab-paclitaxel drives M1 macrophage activation *in vitro*. **A**, Relative gene expression analysis of *Il1a*, *Il1b*, *Il6*, *Il12 p40*, and *Tnfa* normalized to *Gapdh* in RAW 264.7 cells treated with vehicle (DMSO), LPS, paclitaxel (ptx), or nab-paclitaxel (nab-ptx). **B**, Relative gene expression levels of *Il1a*, *Il1b*, *Il6*, *Il12 p40*, and *Tnfa* treated with nab-ptx alone or with EIPA, BAPTA-AM, or anti-CD16/32. **A** and **B**, Bars represent SE from three independent experiments. **C** and **D**, Western blot analysis of iNOS expression in RAW 264.7 cells treated with (C) vehicle (DMSO), IFN $\gamma$ , LPS, ptx or nab-ptx alone, or with IFN $\gamma$ , or (D) vehicle (DMSO), IFN $\gamma$ , nab-ptx, or nab-ptx in combination with IFN $\gamma$  alone or with EIPA. VINCULIN served as a protein loading control. Numbers below Western blots indicate level of iNOS induction normalized to VINCULIN and relative to IFN $\gamma$  alone. All Western blots were cropped using ImageJ to show bands of interest and are representative of at least three independent experiments. Graph in **D** shows relative gene expression *Inos* normalized to *Gapdh* with bars representing SE from four independent experiments. \*,  $P < 0.05$ ; \*\*,  $P < 0.01$ ; ns, not significant.

expression in the tumor-associated M1 population compared with vehicle-treated mice (Fig. 4D). Gene expression analysis of the total macrophage population also revealed a 2-fold increase in

*Il1b* expression following treatment with nab-paclitaxel and gemcitabine (Supplementary Fig. S3C). Together, these data demonstrate that internalization of nab-paclitaxel by pancreatic

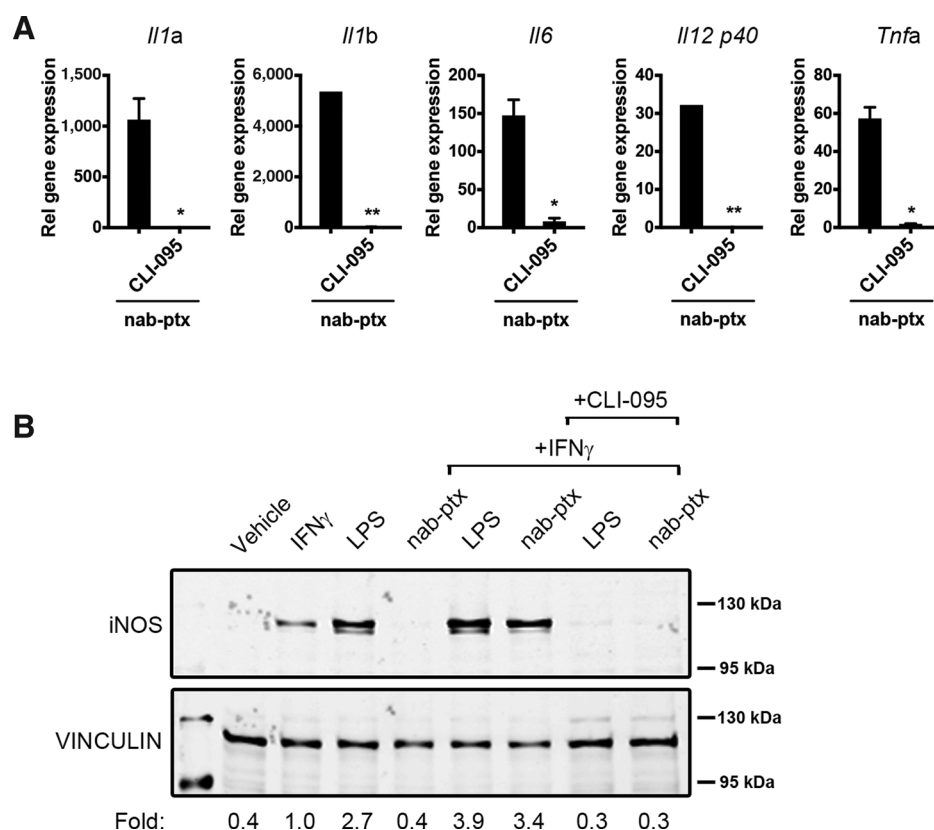


**Figure 3.**

Nab-paclitaxel induces M1 activation in a TLR4-dependent manner. **A**, Relative gene expression levels of *Il1a*, *Il1b*, *Il6*, *Il12 p40*, and *Tnfa* treated with nab-ptx alone or with 500 nm CLI-095. Bars represent SE from three independent experiments. \*,  $P < 0.05$ ; \*\*,  $P < 0.01$ ; ns, not significant. **B**, Western blot analysis of iNOS expression in RAW 264.7 cells treated with vehicle (DMSO), IFN $\gamma$ , or LPS or nab-ptx alone or with IFN $\gamma$  or with IFN $\gamma$  and 25  $\mu\text{mol/L}$  CLI-095.

tumor-associated macrophages can drive them toward an M1 activation state *in vivo*.

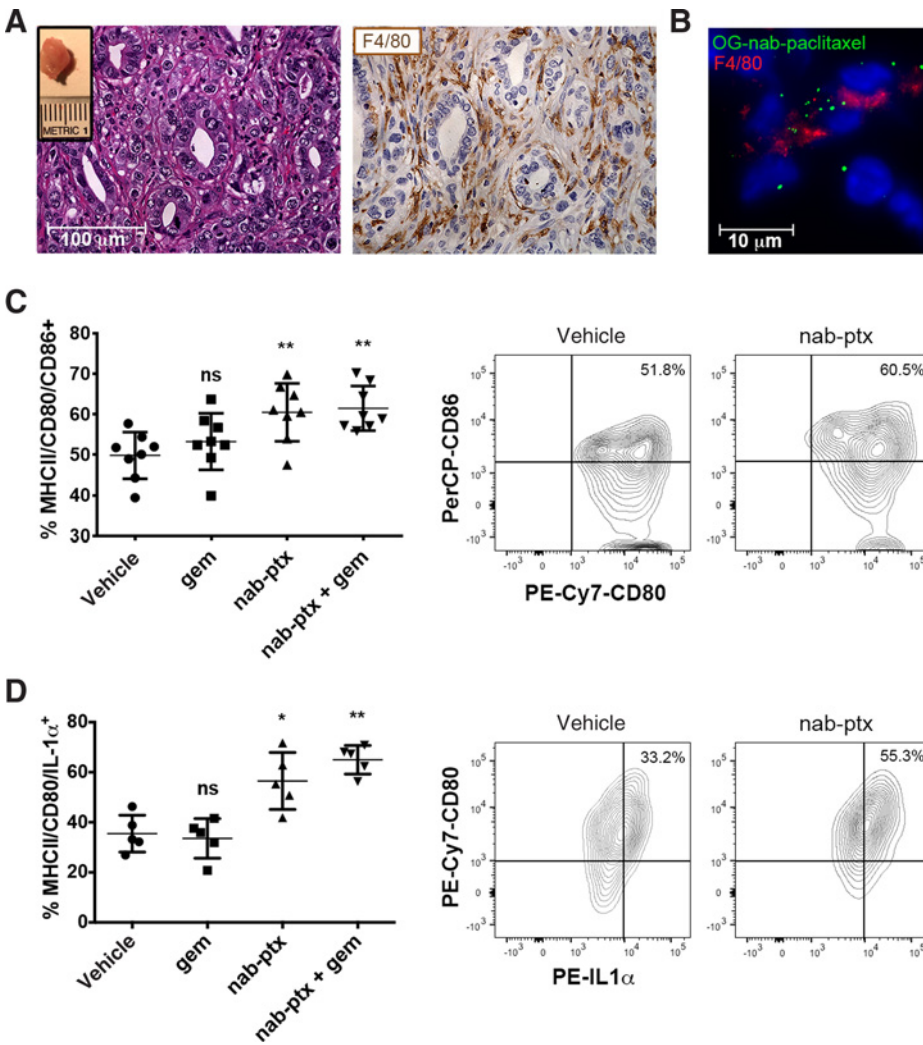
## Discussion

Taxanes, and in particular paclitaxel, represent an important class of antitumor agents that have proven to be effective in the treatment of a number of solid malignancies. The albumin-bound form of paclitaxel, nab-paclitaxel, has fewer side effects, shows increased tumor cell cytotoxicity, and patients have higher overall response rates, compared with equal doses of solvent-based paclitaxel in breast, non-small cell lung (NSCLC), and pancreatic cancers (23). The improved tumor response to nab-paclitaxel has been attributed to elevated intratumoral concentrations mediated by binding of albumin to endothelial 60-kDa glycoprotein receptor (gp60; ref. 24), thereby facilitating vascular transcytosis. It has been proposed that the antitumor activity of nab-paclitaxel might be attributed to its binding to SPARC, a cell surface receptor with sequence homology to gp60 that is expressed on multiple tumor cell types (25, 26). Our findings reported here suggest that nab-paclitaxel-dependent tumor cell killing may be additionally mediated via its immunostimulatory effects on TAMs. The potential relevance of this tumor cell-extrinsic mechanism in the context of PDAC is supported by the observation that paclitaxel provides limited clinical benefit despite exhibiting comparable effects on microtubule function to nab-paclitaxel in tumor cells (27). In murine and human studies of PDAC, nab-paclitaxel more effectively reduces stromal density relative to solvent-based taxanes (27–30). As the activation of pan-

atic stellate cells is influenced by M2 macrophages (31), the stromal-depleting consequences of nab-paclitaxel treatment on the tumor stroma could reflect its effect on macrophage M1 polarization. Both breast cancer and NSCLC, malignancies for which nab-paclitaxel is a standard treatment regimen (23), have extensive immunosuppressive macrophage infiltrates (32, 33). Thus, the proposed mode of action of nab-paclitaxel in promoting macrophage activation might be of broad relevance to tumor sites in which the drug shows therapeutic benefits.

Paclitaxel promotes M1 polarization via direct binding to MD2, an extracellular adaptor protein of TLR4 (18). Upon activation, TLR4 is rapidly internalized into endosomes and engages downstream signaling pathways via endocytic shuttling (34). TLR4 internalization and trafficking is required for efficient LPS-dependent TLR4 signal propagation (34). Although macropinosomes and endosomes are formed as distinct vesicular entities, they fuse in the course of their intracellular trafficking (35). It is therefore plausible that the macropinocytic uptake of nab-paclitaxel enables it to act on endosomal TLR4 complexes. Whether this mode of activation provides the means to increase the local effective concentration of paclitaxel, and/or induce a different signaling repertoire, remains to be established. Inflammatory stimuli, including IFN $\gamma$  and TNF $\alpha$ , induce a shift from phagocytosis to macropinocytosis for the internalization of pathogens by macrophages (36). Nab-paclitaxel-mediated M1 induction may therefore result in positive feedback signaling, promoting further uptake of drug and enhancing its M1-activating effects in both an autocrine and paracrine fashion. Together, these data support the hypothesis that macropinocytosis of the albumin formulation of



**Figure 4.**

Nab-paclitaxel induces M1 activation in pancreatic tumor-associated macrophages *in vivo*. **A**, Representative hematoxylin and eosin (H&E) and F4/80 immunohistochemistry staining of KPC tumors ten days following implantation into syngeneic mice. Inset shows representative dissected KPC tumor. **B**, Cryo-immunofluorescent analysis of orthotopic tumors resected 2 weeks after orthotopic implantation and treated *ex vivo* with 100 μg OG-nab-ptx, followed by immunofluorescent staining with anti-F4/80. Data are representative of three independent experiments. **C**, Quantification of CD80/CD86-positive cells in KPC orthotopic tumors 48 hours after treatment. Left, The CD80<sup>+</sup>CD86<sup>+</sup> cell population was gated on the CD45<sup>+</sup>F4/80<sup>+</sup>MHCII<sup>+</sup> cell population. Data are representative of four independent experiments. Right, Representative FACS plot of CD80<sup>+</sup>CD86<sup>+</sup> cell population from PBS (vehicle; left) and nab-paclitaxel (nab-ptx; right)-treated mice are shown. **D**, Quantification of CD80<sup>+</sup>IL1α<sup>+</sup> cells in KPC orthotopic tumors 48 hours after treatment. Left, CD80<sup>+</sup>IL1α<sup>+</sup> cell population was gated on CD45<sup>+</sup>F4/80<sup>+</sup>MHCII<sup>+</sup> cell population. Right, Representative FACS plot of CD80<sup>+</sup>IL1α<sup>+</sup> cell population from PBS (vehicle; left) and nab-paclitaxel (nab-ptx; right)-treated mice are shown. \*,  $P < 0.05$ ; \*\*,  $P < 0.01$ ; ns, not significant.

paclitaxel promotes its M1-polarizing effects and may account for its elevated activity over solvent-based formulations of paclitaxel. One study suggests that nab-paclitaxel treatment may induce tumor cell toxicity via its internalization and subsequent release by macrophages in the tumor microenvironment (17). However, because a direct uptake of nab-paclitaxel by macrophages was not formally demonstrated in that study, the relevance of this proposed mechanism to our findings that nab-paclitaxel mediates M1 activation cannot be ascertained.

Single-agent immunotherapies designed to activate cytotoxic T cells have shown little benefit in PDAC, despite showing efficacy in many solid tumors (37–39). Given that pancreatic tumor-associated macrophages can contribute to an immunosuppressive microenvironment by inhibiting cytotoxic T-cell function (40), immune recognition may be improved by combining nab-paclitaxel with T-cell immunotherapies. Considering the highly immunocompromised microenvironment of PDAC, however, it is likely that more potent M1 agonists may be required to restore immune surveillance. Several macrophage-activating immunotherapies are in clinical trials for the treatment of a variety of malignancies, including blocking antibodies to colony stimulating factor 1 (41); TLR-activating agents PAM3CSK4 (42) and Poly I:C (43); and

blocking antibodies to IL10 (44). It is possible that coupling such agents to albumin nanoparticles may improve their delivery to macrophages in the tumor microenvironment and more efficiently restore immune recognition. Employing albumin nanoparticles as vehicles for macrophage-activating agents may therefore serve broad applicability in a variety of tumor types exhibiting extensive M2 infiltration.

#### Disclosure of Potential Conflicts of Interest

No potential conflicts of interest were disclosed.

#### Authors' Contributions

**Conception and design:** J. Cullis, A. Maitra, D. Bar-Sagi  
**Development of methodology:** J. Cullis, D. Siolas, S. Barui  
**Acquisition of data (provided animals, acquired and managed patients, provided facilities, etc.):** J. Cullis, D. Siolas, A. Avanzi  
**Analysis and interpretation of data (e.g., statistical analysis, biostatistics, computational analysis):** J. Cullis, D. Siolas, A. Maitra, D. Bar-Sagi  
**Writing, review, and/or revision of the manuscript:** J. Cullis, D. Siolas, A. Maitra, D. Bar-Sagi  
**Study supervision:** D. Bar-Sagi  
**Other (performed *in vivo* experiments):** A. Avanzi  
**Other (chemical synthesis, provided drug formulations):** S. Barui

## Acknowledgments

The authors thank L.J. Taylor and E. Vucic for discussions and help with article preparation. Special thanks to the flow cytometry core for help with flow data acquisition and analysis.

## Grant Support

This work was supported by NIH/NCI grant CA210263 (D. Bar-Sagi) and AACR PanCAN grant 13-90-25-VOND (D. Bar-Sagi). J. Cullis was supported by

NIH grants 5-T32 CA 009161-39 and 5-T32AI100853-04. D. Siolas was supported by NIH grant HL007151-36 and a Schwartz Fellowship.

Received June 7, 2016; revised November 29, 2016; accepted January 4, 2017; published OnlineFirst January 20, 2017.

## References

- Kurahara H, Shinchi H, Mataka Y, Maemura K, Noma H, Kubo F, et al. Significance of M2-polarized tumor-associated macrophage in pancreatic cancer. *J Surg Res* 2011;167:e211-9.
- Mantovani A, Sozzani S, Locati M, Allavena P, Sica A. Macrophage polarization: Tumor-associated macrophages as a paradigm for polarized M2 mononuclear phagocytes. *Trends Immunol* 2002;23:549-55.
- Ino Y, Yamazaki-Itoh R, Shimada K, Iwasaki M, Kosuge T, Kanai Y, et al. Immune cell infiltration as an indicator of the immune microenvironment of pancreatic cancer. *Br J Cancer* 2013;108:914-23.
- Von Hoff DD, Ervin T, Arena FP, Chiorean EG, Infante J, Moore M, et al. Increased survival in pancreatic cancer with nab-paclitaxel plus gemcitabine. *N Engl J Med* 2013;369:1691-703.
- Ding A, Sanchez E, Nathan CF. Taxol shares the ability of bacterial lipopolysaccharide to induce tyrosine phosphorylation of microtubule-associated protein kinase. *J Immunol* 1993;151:5596-602.
- Ding AH, Porteu F, Sanchez E, Nathan CF. Shared actions of endotoxin and taxol on TNF receptors and TNF release. *Science* 1990;248:370-2.
- Perera PY, Mayadas TN, Takeuchi O, Akira S, Zaks-Zilberman M, Goyert SM, et al. CD11b/CD18 acts in concert with CD14 and Toll-like receptor (TLR) 4 to elicit full lipopolysaccharide and taxol-inducible gene expression. *J Immunol* 2001;166:574-81.
- Lo A, Wang LC, Scholler J, Monslow J, Avery D, Newick K, et al. Tumor-promoting desmoplasia is disrupted by depleting FAP-expressing stromal cells. *Cancer Res* 2015;75:2800-10.
- Commisso C, Flinn RJ, Bar-Sagi D. Determining the macropinocytic index of cells through a quantitative image-based assay. *Nat Protoc* 2014;9:182-92.
- Pylayeva-Gupta Y, Lee KE, Hajdu CH, Miller G, Bar-Sagi D. Oncogenic Kras-induced GM-CSF production promotes the development of pancreatic neoplasia. *Cancer Cell* 2012;21:836-47.
- Sallusto F, Cella M, Danieli C, Lanzavecchia A. Dendritic cells use macropinocytosis and the mannose receptor to concentrate macromolecules in the major histocompatibility complex class II compartment: Downregulation by cytokines and bacterial products. *J Exp Med* 1995;182:389-400.
- Lim JP, Gleeson PA. Macropinocytosis: An endocytic pathway for internalising large gulps. *Immunol Cell Biol* 2011;89:836-43.
- Ravetch JV. Fc receptors: Rubor redux. *Cell* 1994;78:553-60.
- Indik ZK, Park JG, Hunter S, Schreiber AD. The molecular dissection of Fc gamma receptor mediated phagocytosis. *Blood* 1995;86:4389-99.
- Di Virgilio F, Meyer BC, Greenberg S, Silverstein SC. Fc receptor-mediated phagocytosis occurs in macrophages at exceedingly low cytosolic Ca<sup>2+</sup> levels. *J Cell Biol* 1988;106:657-66.
- Jongstra-Bilen J, Harrison R, Grinstein S. Fc gamma-receptors induce Mac-1 (CD11b/CD18) mobilization and accumulation in the phagocytic cup for optimal phagocytosis. *J Biol Chem* 2003;278:45720-9.
- Tanei T, Leonard F, Liu X, Alexander JF, Saito Y, Ferrari M, et al. Redirecting transport of nanoparticle albumin-bound paclitaxel to macrophages enhances therapeutic efficacy against liver metastases. *Cancer Res* 2016;76:429-39.
- Zimmer SM, Liu J, Clayton JL, Stephens DS, Snyder JP. Paclitaxel binding to human and murine MD-2. *J Biol Chem* 2008;283:27916-26.
- Stuehr DJ, Nathan CF. Nitric oxide. A macrophage product responsible for cytoxicity and respiratory inhibition in tumor target cells. *J Exp Med* 1989;169:1543-55.
- Lorsbach RB, Murphy WJ, Lowenstein CJ, Snyder SH, Russell SW. Expression of the nitric oxide synthase gene in mouse macrophages activated for tumor cell killing. Molecular basis for the synergy between interferon-gamma and lipopolysaccharide. *J Biol Chem* 1993;268:1908-13.
- Manthey CL, Perera PY, Salkowski CA, Vogel SN. Taxol provides a second signal for murine macrophage tumoricidal activity. *J Immunol* 1994;152:825-31.
- Subauste CS, de Waal Malefyt R, Fuh F. Role of CD80 (B7.1) and CD86 (B7.2) in the immune response to an intracellular pathogen. *J Immunol* 1998;160:1831-40.
- Kundranda MN, Niu J. Albumin-bound paclitaxel in solid tumors: Clinical development and future directions. *Drug Des Devel Ther* 2015;9:3767-77.
- Desai N, Trieu V, Yao Z, Louie L, Ci S, Yang A, et al. Increased antitumor activity, intratumor paclitaxel concentrations, and endothelial cell transport of cremophor-free, albumin-bound paclitaxel, ABI-007, compared with cremophor-based paclitaxel. *Clin Cancer Res* 2006;12:1317-24.
- Desai NP, Trieu V, Hwang LY, Wu R, Soon-Shiong P, Gradishar WJ. Improved effectiveness of nanoparticle albumin-bound (nab) paclitaxel versus polysorbate-based docetaxel in multiple xenografts as a function of HER2 and SPARC status. *Anticancer Drugs* 2008;19:899-909.
- Desai N, Trieu V, Damascelli B, Soon-Shiong P. SPARC expression correlates with tumor response to albumin-bound paclitaxel in head and neck cancer patients. *Transl Oncol* 2009;2:59-64.
- Awasthi N, Zhang C, Schwarz AM, Hinz S, Wang C, Williams NS, et al. Comparative benefits of Nab-paclitaxel over gemcitabine or polysorbate-based docetaxel in experimental pancreatic cancer. *Carcinogenesis* 2013;34:2361-9.
- Alvarez R, Musteanu M, Garcia-Garcia E, Lopez-Casas PP, Megias D, Guerra C, et al. Stromal disrupting effects of nab-paclitaxel in pancreatic cancer. *Br J Cancer* 2013;109:926-33.
- Von Hoff DD, Ramanathan RK, Borad MJ, Laheru DA, Smith LS, Wood TE, et al. Gemcitabine plus nab-paclitaxel is an active regimen in patients with advanced pancreatic cancer: a phase I/II trial. *J Clin Oncol* 2011;29:4548-54.
- DeNardo DG, Barreto JB, Andreu P, Vasquez L, Tawfik D, Kolhatkar N, et al. CD4(+) T cells regulate pulmonary metastasis of mammary carcinomas by enhancing protumor properties of macrophages. *Cancer Cell* 2009;16:91-102.
- Neesse A, Frese KK, Chan DS, Bapiro TE, Howat WJ, Richards FM, et al. SPARC independent drug delivery and antitumor effects of nab-paclitaxel in genetically engineered mice. *Gut* 2014;63:974-83.
- Shi C, Washington MK, Chaturvedi R, Drosos Y, Revetta FL, Weaver CJ, et al. Fibrogenesis in pancreatic cancer is a dynamic process regulated by macrophage-stellate cell interaction. *Lab Invest* 2014;94:409-21.
- Tang X. Tumor-associated macrophages as potential diagnostic and prognostic biomarkers in breast cancer. *Cancer Lett* 2013;332:3-10.
- Ma J, Liu L, Che G, Yu N, Dai F, You Z. The M1 form of tumor-associated macrophages in non-small cell lung cancer is positively associated with survival time. *BMC Cancer* 2010;10:112.
- Latz E, Visintin A, Lien E, Fitzgerald KA, Monks BG, Kurt-Jones EA, et al. Lipopolysaccharide rapidly traffics to and from the Golgi apparatus with the toll-like receptor 4-MD-2-CD14 complex in a process that is distinct from the initiation of signal transduction. *J Biol Chem* 2002;277:47834-43.
- Racoosin EL, Swanson JA. Macropinosome maturation and fusion with tubular lysosomes in macrophages. *J Cell Biol* 1993;121:1011-20.
- Bosedasgupta S, Pieters J. Inflammatory stimuli reprogram macrophage phagocytosis to macropinocytosis for the rapid elimination of pathogens. *PLoS Pathog* 2014;10:e1003879.



38. Brahmer JR, Tykodi SS, Chow LQ, Hwu WJ, Topalian SL, Hwu P, et al. Safety and activity of anti-PD-L1 antibody in patients with advanced cancer. *N Engl J Med* 2012;366:2455–65.
39. Le DT, Lutz E, Uram JN, Sugar EA, Onners B, Solt S, et al. Evaluation of ipilimumab in combination with allogeneic pancreatic tumor cells transfected with a GM-CSF gene in previously treated pancreatic cancer. *J Immunother* 2013;36:382–9.
40. Royal RE, Levy C, Turner K, Mathur A, Hughes M, Kammula US, et al. Phase 2 trial of single agent Ipilimumab (anti-CTLA-4) for locally advanced or metastatic pancreatic adenocarcinoma. *J Immunother* 2010;33:828–33.
41. De Palma M, Lewis CE. Macrophage regulation of tumor responses to anticancer therapies. *Cancer Cell* 2013;23:277–86.
42. Pyonteck SM, Akkari L, Schuhmacher AJ, Bowman RL, Sevenich L, Quail DF, et al. CSF-1R inhibition alters macrophage polarization and blocks glioma progression. *Nat Med* 2013;19:1264–72.
43. Vogelpoel LT, Hansen IS, Rispens T, Muller FJ, van Capel TM, Turina MC, et al. Fc gamma receptor-TLR cross-talk elicits pro-inflammatory cytokine production by human M2 macrophages. *Nat Commun* 2014;5:5444.
44. Cui WY, Zhao S, Polanowska-Grabowska R, Wang J, Wei J, Dash B, et al. Identification and characterization of poly(I:C)-induced molecular responses attenuated by nicotine in mouse macrophages. *Mol Pharmacol* 2013;83:61–72.
45. Guiducci C, Vicari AP, Sangaletti S, Trinchieri G, Colombo MP. Redirecting in vivo elicited tumor infiltrating macrophages and dendritic cells towards tumor rejection. *Cancer Res* 2005;65:3437–46.